Neoplasia • Vol. 8, No. 7, July 2006, pp. 560–567

www.neoplasia.com

The Response of RIF-1 Fibrosarcomas to the Vascular-Disrupting Agent ZD6126 Assessed by *In Vivo* and *Ex Vivo* ^{1}H Magnetic Resonance Spectroscopy[1]

Basetti Madhu, John C. Waterton†, John R. Griffiths*, Anderson J. Ryan‡ and Simon P. Robinson*,[2]*

*Cancer Research UK Biomedical Magnetic Resonance Research Group, St. George's, University of London, London SW17 ORE, UK; †Departments of Imaging, Global Sciences, and Information, AstraZeneca, Alderley Park, Macclesfield, Cheshire SK10 4TG, UK; ‡Cancer and Infection Research, AstraZeneca, Alderley Park, Macclesfield, Cheshire SK10 4TG, UK

Abstract

The response of radiation-induced fibrosarcoma 1 (RIF-1) tumors treated with the vascular-disrupting agent (VDA) ZD6126 was assessed by *in vivo* and *ex vivo* ^{1}H magnetic resonance spectroscopy (MRS) methods. Tumors treated with 200 mg/kg ZD6126 showed a significant reduction in total choline (tCho) *in vivo* 24 hours after treatment, whereas control tumors showed a significant increase in tCho. This response was investigated further within both *ex vivo* unprocessed tumor tissues and tumor tissue metabolite extracts. *Ex vivo* high-resolution magic angle spinning (HRMAS) and ^{1}H MRS of metabolite extracts revealed a significant reduction in phosphocholine and glycerophosphocholine in biopsies of ZD6126-treated tumors, confirming *in vivo* tCho response. ZD6126-induced reduction in choline compounds is consistent with a reduction in cell membrane turnover associated with necrosis and cell death following disruption of the tumor vasculature. *In vivo* tumor tissue water diffusion and lactate measurements showed no significant changes in response to ZD6126. Spin–spin relaxation times (T_2) of water and metabolites also remained unchanged. Noninvasive ^{1}H MRS measurement of tCho *in vivo* provides a potential biomarker of tumor response to VDAs in RIF-1 tumors.

Neoplasia (2006) **8,** 560–567

Keywords: ZD6126, vascular disruption, choline, ^{1}H MRS, HRMAS.

Introduction

A functional vascular network is essential for the survival and growth of solid tumors [1,2]. The dependence of tumor cells on a nutritive blood supply has resulted in the tumor vasculature becoming an attractive therapeutic target. Vascular-disrupting agents (VDAs) have been developed to exploit differences between normal and tumor vascular endothelium, with the aim of selectively destroying tumor blood vessels while leaving normal vessels unaffected [3,4]. *N*-acetylcolchinol-*O*-phosphate (ZD6126) is a small-molecule VDA that is shown to have significant antitumor activity against rodent and human tumor model systems [5–9] and against human tumor vasculature [10]. It is a water-soluble phosphate prodrug of the tubulin-binding agent *N*-acetylcolchinol that inhibits tubulin polymerization, disrupting the microtubule cytoskeleton [11]. Following ZD6126 treatment, disruption of the tubulin cytoskeleton in proliferating endothelial cells leads to endothelial cell detachment, tumor vascular shutdown, and, ultimately, massive central hemorrhagic necrosis [5,6]. A surviving rim of tumor cells is characteristically seen histologically following treatment. As a consequence, VDAs characteristically induce tumor growth delay but not tumor regression, as the tumor regrows from this viable rim. Thus, the clinical development of VDAs will be greatly assisted by the use of biomarkers that are sensitive to disrupted tumor perfusion. To this end, noninvasive imaging methods, such as magnetic resonance imaging (MRI) [9,10] and positron emission tomography [12], are being exploited.

Magnetic resonance spectroscopy (MRS) methods provide noninvasive measurements of tumor biochemistry. Localized *in vivo* ^{1}H MRS techniques have been developed to quantify the concentration (in mM) of tumor total choline (tCho; an important metabolic marker that is associated with membrane turnover, malignancy, and tumor grade) [13–15] and lactate (another significant tumor metabolite that is associated with

Abbreviations: ADC, apparent water diffusion coefficient; DDC, distributed diffusion coefficient; GPC, glycerophosphocholine; HRMAS, high-resolution magic angle spinning; i.p., intraperitoneal; MRS, magnetic resonance spectroscopy; PC, phosphocholine; tCho, total choline; tCr, total creatine; VDA, vascular-disrupting agent

Address all correspondence to: Dr. Basetti Madhu, Cancer Research UK Biomedical MR Research Group, Division of Basic Medical Sciences, St. George's, University of London, Cranmer Terrace, London SW17 0RE, UK. E-mail: mbasetti@sgul.ac.uk

[1]This work was supported by Cancer Research UK, grant C12/A1209, AstraZeneca, and The Royal Society. S.P.R. is the recipient of a Royal Society University research fellowship.

[2]Present address: Cancer Research UK Clinical Magnetic Resonance Research Group, Institute of Cancer Research and Royal Marsden NHS Trust, Cotswold Road, Sutton, Surrey SM2 5PT, UK.

Received 24 April 2006; Revised 25 May 2006; Accepted 26 May 2006.

DOI 10.1593/neo.06319

glycolysis, acidosis, and hypoxia) [13–17]. Choline, phosphocholine (PC), and glycerophosphocholine (GPC) all contribute to the tCho trimethylamino resonance detected at 3.23 ppm, but they cannot be individually resolved *in vivo* due to the typically low magnetic field homogeneity achievable *in vivo*. To understand the individual contributions of choline compounds to *in vivo* tCho resonance, both high-resolution magic angle spinning (HRMAS) ^{1}H MRS, from which well-resolved spectra can be obtained from a few milligrams of unprocessed solid tumor samples [18–20], and ^{1}H MRS of sequential tumor metabolite extractions have been used [21].

Water diffusion within tumors is another property of tumors that is currently being intensively investigated. Apparent water diffusion coefficient (ADC), measured *in vivo* by ^{1}H MRS, is sensitive to the biophysical characteristics of tissues, including the fraction of extracellular space. Several studies have shown the potential of ADC as a biomarker of therapeutic response in tumors [22–25].

We have previously shown that 200 mg/kg ZD6126 induces massive hemorrhagic necrosis in RIF-1 tumors 24 hours after treatment [9]. The aims of this study were to investigate the utility of *in vivo* ^{1}H MRS to provide biomarkers of response to ZD6126 in RIF-1 tumors, and to provide any validation of these biomarkers with *ex vivo* HRMAS and ^{1}H MRS of tumor extracts following treatment.

Methods

Animals and Tumors

All experiments were performed in accordance with the local ethical review panel, the UK Animals (Scientific Procedures) Act 1986, and the United Kingdom Coordinating Committee on Cancer Research guidelines [26]. Murine radiation-induced fibrosarcoma 1 (RIF-1) was grown subcutaneously in the flanks of C3H female mice (n = 12) [27]. Tumor volume was calculated by measuring length (l), width (w), and depth (d) using calipers and the formula: $lwd(\pi / 6)$.

Administration of Anesthesia and Dosage of ZD6126

The mice were anesthetized with a 10-ml/kg intraperitoneal (i.p.) injection of fentanyl citrate (0.315 mg/ml) plus fluanisone (10 mg/ml) (Hypnorm; Janssen Pharmaceutical Ltd., Oxford, UK), midazolam (5 mg/ml) (Hypnovel; Roche, Welwyn Garden City, Herts, UK), and water (1:1:2). ZD6126 was obtained from AstraZeneca (Cheshire, UK) and formulated in 20% of 5% sodium carbonate and 80% phosphate-buffered saline, yielding a clear solution at *ca.* pH 7.

In Vivo ^{1}H MRS

Anesthetized mice were placed in the bore of a 4.7-T horizontal magnet fitted with a 10-G/cm 12-cm-bore high-performance auxiliary gradient insert interfaced to a Varian Unity Inova spectrometer (Varian Instruments, Palo Alto, CA), so that the tumors hung on a two-turn ^{1}H radiofrequency coil of 15 mm diameter. Body temperature was maintained with a water-heated pad placed over the mouse. Voxels were selected from scout gradient echo images, and localized shimming yielded linewidths on the order of 20 to 30 Hz. PRESS localization with water suppression was used to detect choline, with a repetition time of 2 seconds, 64 transients, and echo times of 20, 68, 136, 272, and 408 milliseconds. Water suppression included selective excitation of water signal by 14-millisecond Gaussian pulse followed by dephasing gradients in three orthogonal directions in repetition time delay. For unsuppressed water, 16 transients were acquired with the same acquisition parameters as above, except with a lower receiver gain. A multiple quantum coherence (MQC) editing sequence with a single-shot outer volume–saturated localization [28] and a repetition time of 3 seconds was used to detect lactate signal. A localized STEAM sequence with diffusion-sensitizing gradients in echo-time periods was used to separately obtain diffusion-weighted (DW) ^{1}H MRS data for each orthogonal (x, y, z) direction. The acquisition parameters for DW-MRS were T_E = 24 milliseconds, T_M = 100 milliseconds, T_R = 3 seconds, δ = 6 milliseconds, and Δ = 112 milliseconds, with diffusion gradients increasing from 0 to 13 G/cm with a 1-G/cm interval. Corresponding b values were 0, 2731, 10,924, 24,579, 43,696, 68,276, 98,317, 133,820, 174,786, 221,214, 273,104, 330,455, 393,269, and 461,545 sec/cm^2.

After pretreatment ^{1}H MRS measurements, saline or 200 mg/kg ZD6126 was administered intraperitoneally, and ^{1}H MRS was repeated 24 hours later. Immediately after posttreatment *in vivo* MRS measurements, anesthetized mice were sacrificed by cervical dislocation and the tumors were rapidly excised and either frozen intact for HRMAS MRS or freeze-clamped in liquid nitrogen for high-resolution ^{1}H MRS of tissue extracts.

In Vivo ^{1}H MRS Data Analysis

MRUI software [29], using the AMARES [30] algorithm in the time domain, was used for data processing and resonance fitting. The method included metabolite lineshape correction and zero-order phasing using a water reference signal [31], removal of residual water signal in the range of 4.5 to 5.0 ppm using Hankel Lanczos Singular Value Decomposition, and direct current offset calculated from the last 100 data points. The first data point in free induction decay was excluded to minimize the contribution from broad signals underlying the whole spectrum, which, when present, can result in an overestimation of metabolite signals. Gaussian lineshapes were assumed for the estimation of metabolite peak areas. Prior knowledge used to constrain fitting parameters included the application of equal linewidths of tCho and total creatine (tCr; creatine plus phosphocreatine) resonances (with the assumption that shimming dominates linewidth) [17], and also that the chemical shifts of metabolite resonances were limited to 0.05 ppm about their expected values of 3.22 and 3.03. The tCho, tCr, and water peak areas were plotted as a function of echo time, and the intercept (M_0) and metabolite T_2 values were determined by assuming a monoexponential decay function using the Levenberg-Marquardt algorithm.

Metabolite concentrations were calculated using tumor water as a reference, assuming tissue water was 80% (88 M protons), according to the equation [13,14]:

$$[\text{metabolite}] = (\text{metabolite/water})_{T_E=0} W_c (N_w/N_m)(AV_n RG_c)$$

where [metabolite] = metabolite concentration; $(\text{metabolite/water})_{T_{E=0}}$ = ratio of metabolite and water intercepts at $T_E = 0$, as determined from individual T_2 fits; W_c = water concentration (44 M); N_w = number of protons in water (2); N_m= number of protons contributing to metabolite resonance (for tCho, N_m= 9; for tCr, N_m = 3); AV_n = normalization factor for the number of averages; and RG_c = receiver gain correction factor. The corrections for the number of averages and receiver gains were needed because they were different for the acquisition of water and metabolite spectra. Quantitation of lactate was not possible because the signal observed with the MQC editing sequence was acquired at a fixed echo time; thus, an uncorrected lactate/water signal ratio was determined using water intercept values calculated from T_2 curves at $T_E = 0$.

For analysis of diffusion-weighted data, the plots of normalized water signal (M/M_0) against b values were fitted with a stretched exponential model [$M/M_0 = \exp\{-(b\text{DDC})^{\alpha}\}$], resulting in the estimation of a heterogeneity index (α) and distributed diffusion coefficient (DDC) [32]. The Levenberg-Marquardt algorithm was used for optimization. The average values of DDC and α were estimated by $\text{DDC} = (\text{DDC}_{xx} + \text{DDC}_{yy} + \text{DDC}_{zz})/3$ and $\alpha = (\alpha_{xx} + \alpha_{yy} + \alpha_{zz})/3$.

HRMAS ^{1}H MRS

Frozen tumor tissue (12 ± 3 mg) was transferred to a 4-mm zirconium oxide HRMAS rotor. Deuterium oxide (10 μl) was added for field frequency locking. All HRMAS experiments were performed on a 600-MHz (14.1-T) Bruker AVANCE spectrometer (Bruker Biospin, Coventry, UK) with a spin rate of 4000 ± 2 Hz at 277 K. Spectra were acquired with a CPMG pulse sequence [$90 - (\tau - 180)_n - \tau -$ acq] as a T_2 filter to remove broad resonances arising from slowly tumbling macromolecules and lipids. The interpulse delay τ was 250 microseconds, and spectra were obtained with 128 transients, 32,000 data points, and 8 kHz spectral width. The 90° pulse was adjusted for individual samples and varied from 13.5 to 14.5 microseconds. T_2 measurements were performed by varying the effective T_2 filter time from 100 to 1000 milliseconds in six increments. Spectral processing included 0.5-Hz apodization, Fourier transformation, and first-order phase correction. A monoexponential decay of metabolite signal with echo time was assumed to estimate equilibrium magnetization (M_0) and T_2 values of metabolites. M_0 was used for quantitation of metabolites. The creatine peak at 3.03 ppm was used as a chemical shift reference [20]. tCr content [tCr = creatine (Cr) + phosphocreatine (PCr)], which was obtained from the total extracted by perchloric acid (PCA), methanol, and chloroform extractions (see later) for each tumor, was used as an internal standard for the quantitation of metabolites by HRMAS [20].

High-Resolution ^{1}H MRS of Tissue Extracts

Tissue metabolites from frozen tissue were extracted using PCA and methanol/chloroform methods [21]. Frozen tumor tissue was ground to a fine powder using mortar and pestle. One part of tissue plus four parts of 6% PCA were homogenized and centrifuged, and the resulting supernatant was neutralized. After lyophilization, the sample was used for high-resolution ^{1}H MRS. Methanol and chloroform (2:1; 3 ml/g) were added to the residual pellet (after PCA extraction) and homogenized. The mixture was left on ice for 15 minutes, and then chloroform and distilled water (1:1; 1 ml/g) were added to form an emulsion. Centrifuging the sample resulted in a clear separation of the upper (methanol and water) phase from the lower organic (chloroform) phase, with the pellet in the middle. Both phases were carefully separated and dried at room temperature. All dried samples were then reconstituted in 1 ml of deuterium oxide, except for chloroform-extracted metabolites that were taken up in 1 ml of $CDCl_3$, and 0.5 ml of this sample was placed in a 5-mm standard nuclear magnetic resonance tube. Sodium 3-trimethylsilyl-2,2,3,3-tetradeuteropropionate (50 μl, 5 mM) was added as an external standard for chemical shift calibration and quantitation of metabolites. Immediately before MRS analysis, the pH of the samples was readjusted to 7 with PCA or potassium hydroxide. All high-resolution ^{1}H MRS data were acquired at 600 MHz (14.1 T) using a Bruker AVANCE spectrometer. ^{1}H MRS acquisition included presaturation of water using gated irradiation centered on water frequency, a repetition time of 5 seconds, and 128 averages.

Results

Irrespective of treatment, the tumor volume of all RIF-1 tumors significantly increased over the 24-hour period of study (Table 1). Localized PRESS ^{1}H MRS yielded a well-resolved tCho resonance at 3.23 ppm and a tCr resonance at 3.03 ppm in all RIF-1 tumors *in vivo*. Representative spectra from one RIF-1 tumor before and after treatment with 200 mg/kg ZD6126 are shown in Figure 1. Lactate signals were also detected in both pretreatment and post-treatment MQC ^{1}H spectra.

Individual tCho concentrations for all RIF-1 tumors before and 24 hours after treatment with either saline or 200 mg/kg ZD6126 are shown in Figure 2. All saline-treated tumors showed an increase in tCho, whereas tCho decreased in all ZD6126-treated tumors. The individual tumor tCho concentrations before and after treatment with either saline or ZD6126, plotted as a function of tumor volume, are shown in Figure 3. The *in vivo* ^{1}H MRS data obtained from RIF-1 tumors are summarized in Table 1. A significant (P = .009) reduction in the tCho of RIF-1 tumors was determined 24 hours after treatment with ZD6126, whereas tCho significantly increased over 24 hours in saline-treated control tumors. There were no significant changes in water T_2, tCho T_2, tCr T_2, and lactate/water ratio in either control or treated cohorts. *In vivo* water DDC and the heterogeneity index α showed no change in either saline-treated or ZD6126-treated cohorts.

Table 1. Summary of *In Vivo* ^{1}H MRS Data Obtained from RIF-1 Tumors before and 24 Hours after Treatment with Either Saline (n = 6) or 200 mg/kg ZD6126 (n = 6).

Variable	Saline		ZD6126	
	Pretreatment	Posttreatment	Pretreatment	Posttreatment
Volume (mm^3)	458 ± 65	589 ± 85*	518 ± 52	671 ± 57†
tCho (mM)	4.43 ± 0.20	5.09 ± 0.17*	5.73 ± 0.46	2.40 ± 0.51*
tCr (mM)	4.81 ± 0.38	5.14 ± 0.76	4.56 ± 0.73	3.14 ± 0.57
Water T_2 (milliseconds)	53.3 ± 1	52.8 ± 2	51.4 ± 1	46.9 ± 4
tCho T_2 (milliseconds)	190 ± 13	157 ± 17	162 ± 14	142 ± 12
tCr T_2 (milliseconds)	142 ± 12	133 ± 16	138 ± 12	116 ± 13
Lactate/water ($\times 10^{-3}$)	3.79 ± 0.80	3.08 ± 0.95	3.06 ± 0.82	1.54 ± 0.68
DDC ($\times 10^{-6}$ cm^2/sec)	5.39 ± 0.45	5.17 ± 0.48	4.72 ± 0.28	5.63 ± 1.30
Heterogeneity index (α)	0.77 ± 0.03	0.77 ± 0.01	0.75 ± 0.02	0.75 ± 0.02

Values are mean ± SEM.
*P < .02, Student's paired t test between pretreatment and posttreatment values.
†P < .05, Student's paired t test between pretreatment and posttreatment values.

The metabolite concentrations determined from unprocessed tumor tissue by HRMAS ^{1}H MRS and from high-resolution ^{1}H MRS of tissue extracts are summarized in Table 2. Both methods revealed a significant reduction in PC and GPC, but no change in free choline concentrations, in ZD6126-treated RIF-1 tumors. The sum of free choline, PC, and GPC (the metabolites that contribute to tCho resonance detected *in vivo*) was calculated for each MRS method for comparison of *in vivo* and *ex vivo* tCho data. A highly significant reduction in tCho was found in ZD6126-treated unprocessed tumor tissue by HRMAS, but not in tissue extracts determined by high-resolution ^{1}H MRS. Both *ex vivo* MRS methods revealed a significant reduction in tCr and taurine following treatment with ZD6126. Alanine was also found to be significantly reduced, as determined by HRMAS ^{1}H MRS only. There were no significant changes in the concentration of lactate, glycine, or acetate.

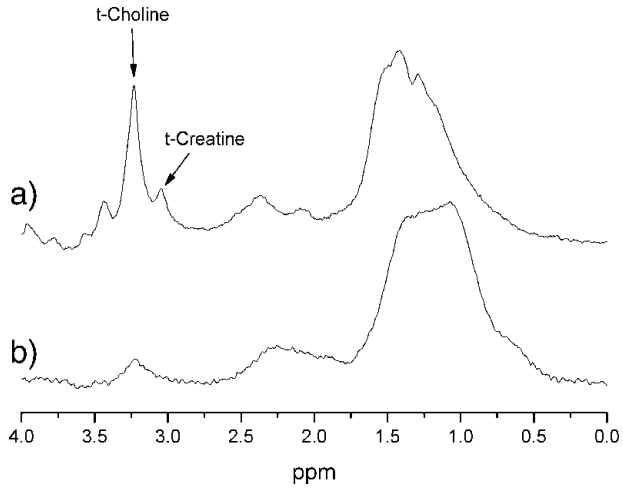

Figure 1. *In vivo PRESS-localized ^{1}H MRS spectra (T_E = 136 milliseconds) acquired from one RIF-1 tumor (a) before and (b) 24 hours posttreatment with 200 mg/kg ZD6126.*

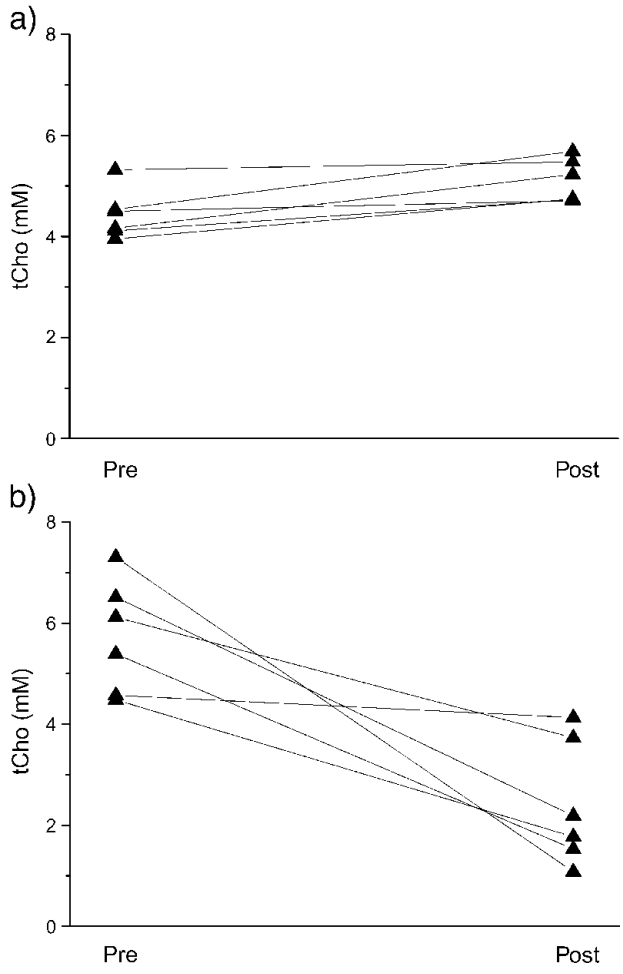

Figure 2. *Line series of tCho concentration (mM) determined by in vivo ^{1}H MRS for each RIF-1 tumor (a) before and 24 hours after saline, and (b) before and 24 hours after 200 mg/kg ZD6126, i.p.*

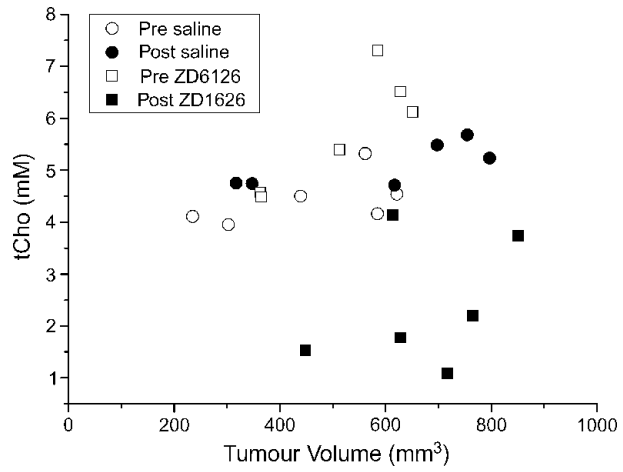

Figure 3. *tCho concentration plotted as a function of tumor volume for each individual RIF-1 tumor investigated by in vivo ^{1}H MRS.*

Table 2. Tumor Metabolite Concentrations (μmol/kg) Determined by ^{1}H HRMAS of Unprocessed Tissues and by High-Resolution ^{1}H MRS of Tissue Extracts of RIF-1 Tumors 24 Hours after Treatment with Saline (n = 6) or 200 mg/kg ZD6126 (n = 6).

Metabolite	HRMAS		Extracts	
	Saline	ZD6126	Saline	ZD6126
Choline	1.94 ± 0.3	1.11 ± 0.4	3.23 ± 0.8	2.96 ± 0.8
PC	2.34 ± 0.3	0.65 ± 0.3*	1.03 ± 0.2	0.36 ± 0.03*
GPC	1.80 ± 0.2	0.52 ± 0.1*	1.34 ± 0.2	0.74 ± 0.11†
tCho	6.08 ± 0.8	2.28 ± 0.5*	5.60 ± 0.7	4.07 ± 0.7
PC/GPC	1.32 ± 0.07	1.32 ± 0.42	0.82 ± 0.14	0.58 ± 0.15
Lactate	34.2 ± 11	14.02 ± 2.5	6.24 ± 0.92	7.70 ± 0.73
Alanine	4.34 ± 0.5	2.15 ± 0.46*	2.77 ± 0.3	2.17 ± 0.3
tCr	2.94 ± 0.3	1.55 ± 0.4*	2.94 ± 0.3	1.55 ± 0.4*
Taurine	16 ± 1.8	4.7 ± 1.4*	7.8 ± 0.3	3.07 ± 0.98*
Glycine	3.48 ± 0.31	2.53 ± 0.7	2.35 ± 0.18	1.51 ± 0.41
Acetate	0.73 ± 0.09	0.55 ± 0.15	0.94 ± 0.17	1.21 ± 0.10

Values are mean ± SEM.
*P < .02, Student's t test.
†P < .05, Student's t test.

A comparison of the tCho concentrations of RIF-1 tumors determined 24 hours after saline or ZD6126 by *in vivo* ^{1}H MRS, HRMAS ^{1}H MRS, and high-resolution ^{1}H MRS of tissue extracts is shown in Figure 4. The *ex vivo* data measured in micromoles per gram per wet weight were converted to millimolars by dividing by a factor of 0.80 (mM = μmol/g per wet weight per 0.8) to allow for a comparison with the *in vivo* ^{1}H MRS data measured in millimolars [18,33]. Both *in vivo* and HRMAS ^{1}H MRS, but not high-resolution ^{1}H MRS of tumor extracts, revealed a significant reduction in tCho concentration in ZD6126-treated tumors. Figure 5 summarizes the tCho/tCr ratios for saline-treated and ZD6126-treated tumors, as determined by *in vivo* ^{1}H MRS, HRMAS ^{1}H MRS, and high-resolution ^{1}H MRS of tissue extracts. There was no significant difference in the tCho/tCr ratio in response to ZD6126 measured by the three different ^{1}H MRS methods.

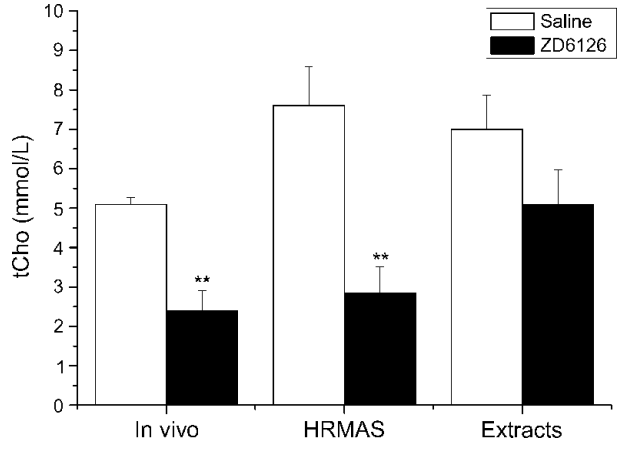

Figure 4. *tCho concentrations (mM) determined by in vivo ^{1}H MRS of unprocessed tissues, by HRMAS ^{1}H MRS of extracts, and by HR ^{1}H MRS of tissue extracts of RIF-1 tumors 24 hours after treatment with saline or 200 mg/kg ZD6126. tCho determined in vivo and by HRMAS was significantly reduced (**P < .02).*

Discussion

The aim of this study was to investigate the use of *in vivo* ^{1}H MRS to assess the metabolic status of RIF-1 tumors before and 24 hours after treatment with 200 mg/kg ZD6126, a dose and timing regime previously shown to induce massive hemorrhagic tumor necrosis in this murine model [9]. Validation of *in vivo* response was sought using HRMAS ^{1}H MRS and high-resolution ^{1}H MRS of tissue extracts. In addition, the biophysical properties of tumor water T_2, diffusion, and their response to ZD6126 were also investigated.

Metabolite Response to ZD6126

A common observation in MRS studies of cancer is elevation in the concentration of choline metabolites, although the precise reasons for this are still unclear [34]. It has been traditionally attributed to an increased biosynthesis of membranes by rapidly proliferating tumor cells [35], and the significant increase in the tCho concentration of control RIF-1 tumors over 24 hours reported herein is consistent with this. Recent evidence suggests that, in addition to biosynthetic pathways, mitogen-induced and oncogene-induced activation of phosphatidylcholine and phosphatidylethanolamine metabolism can increase the accumulation of choline metabolites in tumor cells [36]. Upregulation of choline kinase, which catalyzes the phosphorylation of choline to yield PC, may also contribute [37].

The significant decrease in tCho concentration of RIF-1 tumors *in vivo* 24 hours after treatment with ZD6126, which was observed despite continued tumor growth (Figure 3), is consistent with reduced cell membrane turnover associated with necrosis following disruption of the tumor vasculature. This *in vivo* response biomarker was further validated by a significant ZD6126-induced decrease in both PC and GPC (key metabolites associated with membrane biosynthesis that contribute to tCho resonance detected *in vivo*), as measured by HRMAS ^{1}H MRS and high-resolution ^{1}H MRS of tissue extracts. Quantitative ^{1}H MRS revealed a similar response pattern of HT29 tumors after treatment with the VDA

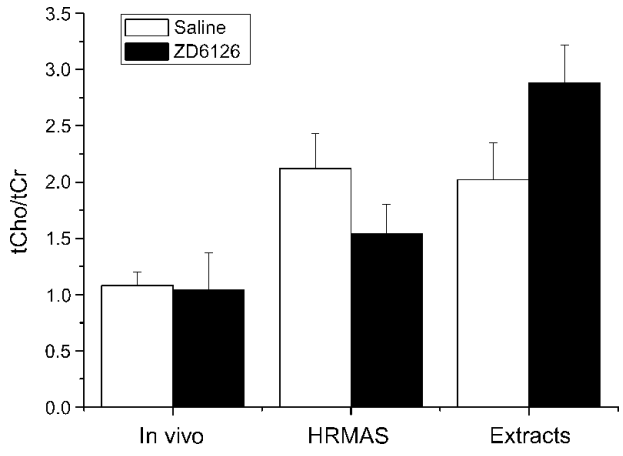

Figure 5. *tCho/tCr ratios of RIF-1 tumors determined by in vivo ^{1}H MRS, HRMAS ^{1}H MRS, and high-resolution ^{1}H MRS of tissue extracts 24 hours after treatment with either saline or 200 mg/kg ZD6126.*

5,6-dimethylxanthenone acetic acid (DMXAA) [13]. A significant reduction in tCho concentration was found 24 hours after treatment with 21 mg/kg DMXAA. Metabolite ratios, derived from *in vivo* ^{1}H MRS, showed a significant reduction in tCho/water of C3H mammary carcinomas 24 hours after treatment with 250 mg/kg combretastatin A4 phosphate (CA4P), another VDA [38,39].

The difficulty of acquiring quantitative metabolite concentrations using volume-selective *in vivo* ^{1}H MRS has resulted in metabolite ratios being reported as surrogate markers of tumor metabolism and response. Intriguingly, the tCho/tCr ratio determined *in vivo* by HRMAS ^{1}H MRS and high-resolution ^{1}H MRS of tumor extracts showed no significant change following treatment with ZD6126. One possible explanation is that ZD6126-induced necrosis and cell death reduce cell density, resulting in the reduction of both tCho and tCr concentrations (hence, no change in their ratio). This highlights the need for caution when using metabolite ratios as biomarkers of response to therapy.

We initially hypothesized that the tumor lactate/water ratio would increase as a result of hypoxia/acidosis induced by ZD6126-induced vascular shutdown. However, there was no significant change in this ratio—a finding similar to that reported for C3H mammary carcinomas 24 hours after treatment with 250 mg/kg CA4P [38]. Experiments using ^{14}C-labeled ZD6126 have shown that the VDA itself is cleared from tumors within 24 hours of administration (A. J. Ryan, personal communication). Lactate is a molecule smaller than ZD6126 and is readily extruded from tumor cells [40]; thus, it is reasonable to assume that any lactate produced following treatment with ZD6126 is largely cleared from the tumor within 24 hours, hence the absence of any significant changes in the tumor lactate/water ratio.

Both HRMAS ^{1}H MRS and high-resolution ^{1}H MRS of tissue extracts showed a significant reduction in the taurine concentration of ZD6126-treated RIF-1 tumors. Taurine is an important organic osmolyte in mammalian cells and is abundant in skeletal muscles [41]. A recent study showed that ZD6126 treatment reduces tumor interstitial fluid pressure [42]; thus, reduction in taurine may reflect a change in pressure gradients and reduced fluid movement through the tumor interstitium associated with the induction of cell death and necrosis.

Tumor Biophysical Response to ZD6126

The majority of anticancer chemotherapeutic drugs kill cells by inducing either apoptosis or necrosis. In either process, the tissue microenvironment is altered by a reduction in intracellular space and a subsequent increase in extracellular space. Quantitation of the spin–spin relaxation time T_2 of water, tCho, and tCr revealed no significant change irrespective of treatment determined *in vivo* (Table 1) or by HRMAS ^{1}H MRS (data not shown). A small (*ca.* 20%) yet significant increase in the T_2 of water in rat GH3 prolactinomas, as quantified by MRI 24 hours after treatment with ZD6126, was recently reported and attributed to edema [43]. No significant change in T_2-weighted image intensity of C3H mammary carcinomas was reported 24 hours post-treatment with CA4P [38]. We also hypothesized that ZD6126-induced hemorrhagic necrosis would result in an increase in extracellular space and, thus, in water diffusion biomarkers. Instead, we found no significant changes in DDC or tumor heterogeneity index (α) *in vivo*, suggesting no significant changes in the biophysical characteristics of the tumor tissue 24 hours after treatment. A similar observation was recently reported in murine RIF-1 tumors treated with 200 mg/kg ZD6126, in which there was no significant change in the apparent diffusion coefficient (ADC) of tumors 24 hours posttreatment, but subsequent significant increases in ADC at 48 and 72 hours posttreatment [44]. A significant increase in the ADC of rat rhabdomyosarcomas 48 hours after treatment with CA4P has also been reported [25]. Together, these data suggest that any VDA-induced changes in the biophysical structure of the tumor tissue occur relatively slowly and are preceded by changes in tumor metabolism.

Utility of MRS Biomarkers of Tumor Response

As a consequence of their inability to induce tumor regressions, the development of VDAs has necessitated the identification of sensitive biomarkers of tumor vascular disruption. In this regard, ^{1}H MRI methods, with their high spatial and temporal resolutions, are attractive, and the biomarkers K^{trans} (the transfer constant describing the transendothelial transport of a low-molecular-weight contrast agent into the extravascular extracellular space) and IAUGC (the initial area under the gadolinium concentration–time curve), derived from dynamic contrast-enhanced MRI, are particularly suited for VDA evaluation in both preclinical and human tumors [45]. Preclinical *in vivo* MRS methods have also been applied to assess tumor response to VDAs. Both ^{31}P MRS and ^{1}H MRS have shown dramatic reductions in tumor energetics and cell membrane proliferation in response to VDAs, and have highlighted the potential of the βNTP/Pi ratio and tCho as early biomarkers of tumor response to this class of drug [13,38,39,46,47]. Similar MRS methods have also been used for the preclinical assessment of other novel targeted cancer therapeutics, and it is clear from these studies that the determination of tCho by ^{1}H MRS *in vivo* also provides a robust biomarker of tumor response [14,48], in contrast to those derived by ^{31}P MRS where evidence of objective tumor response is unclear [14,49]. Recently, ^{1}H MRS has been successfully used in the clinic to quantify tCho concentrations of locally advanced breast cancer before and after neoadjuvant chemotherapy to predict response [15]. Significant reductions in tCho were reported post-treatment, further highlighting the potential utility of tCho as a biomarker of tumor response.

In conclusion, we have shown that quantitation of tCho by ^{1}H MRS *in vivo* is a sensitive biomarker of both the progression and the response of RIF-1 tumors to the VDA ZD6126. Tumor tCho concentration was significantly reduced 24 hours after treatment with 200 mg/kg ZD6126 and appeared to precede any changes in the biophysical properties of the tissue. HRMAS ^{1}H MRS and high-resolution ^{1}H MRS of tissue extracts showed significant reductions in the concentration of PC and GPC (constituents of the tCho

resonance detected *in vivo*), thereby validating tCho response. Quantitation of tCho (mM) by *in vivo* ^{1}H MRS may provide a noninvasive biomarker of early tumor response to VDAs.

Acknowledgements

The authors would like to thank Glyn Fisher and his staff for care of the animals.

References

[1] Folkman J (1985). Tumor angiogenesis. *Adv Cancer Res* **43,** 175–203.
[2] Carmeliet P (2003). Angiogenesis in health and disease. *Nat Med* **9,** 653–660.
[3] Siemann DW, Chaplin DJ, and Horsman MR (2004). Vascular-targeting therapies for treatment of malignant disease. *Cancer* **100,** 2491–2499.
[4] Tozer GM, Kanthou C, and Baguley BC (2005). Disrupting tumour blood vessels. *Nat Rev Cancer* **5,** 423–435.
[5] Blakey DC, Westwood FR, Walker M, Hughes GD, Davis PD, Ashton SE, and Ryan AJ (2002). Antitumor activity of the novel vascular targeting agent ZD6126 in a panel of tumor models. *Clin Cancer Res* **8,** 1974–1983.
[6] Davis PD, Dougherty GJ, Blakey DC, Galbraith SM, Tozer GM, Holder AL, Naylor MA, Nolan J, Stratford MR, Chaplin DJ, and Hill SA (2002). ZD6126: a novel vascular-targeting agent that causes selective destruction of tumor vasculature. *Cancer Res* **62,** 7247–7253.
[7] Siemann DW and Rojiani AM (2002). Enhancement of radiation therapy by the novel vascular targeting agent ZD6126. *Int J Radiat Oncol Biol Phys* **53,** 164–171.
[8] Siemann DW and Rojiani AM (2002). Antitumor efficacy of conventional anticancer drugs is enhanced by the vascular targeting agent ZD6126. *Int J Radiat Oncol Biol Phys* **54,** 1512–1517.
[9] Robinson SP, McIntyre DJ, Checkley D, Tessier JJ, Howe FA, Griffiths JR, Ashton SE, Ryan AJ, Blakey DC, and Waterton JC (2003). Tumour dose response to the antivascular agent ZD6126 assessed by magnetic resonance imaging. *Br J Cancer* **88,** 1592–1597.
[10] Evelhoch JL, LoRusso PM, He Z, DelProposto Z, Polin L, Corbett TH, Langmuir P, Wheeler C, Stone A, Leadbetter J, et al. (2004). Magnetic resonance imaging measurements of the response of murine and human tumors to the vascular-targeting agent ZD6126. *Clin Cancer Res* **10,** 3650–3657.
[11] Micheletti G, Poli M, Borsotti P, Martinelli M, Imberti B, Taraboletti G, and Giavazzi R (2003). Vascular-targeting activity of ZD6126, a novel tubulin-binding agent. *Cancer Res* **63,** 1534–1537.
[12] Laking GR and Price PM (2003). Positron emission tomographic imaging of angiogenesis and vascular function. *Br J Radiol* **76,** S50–S59.
[13] McPhail LD, Chung YL, Madhu B, Clark S, Griffiths JR, Kelland LR, and Robinson SP (2005). Tumor dose response to the vascular disrupting agent, 5,6 dimethylxanthenone-4-acetic acid, using *in vivo* magnetic resonance spectroscopy. *Clin Cancer Res* **11,** 3705–3713.
[14] Al-Saffar NM, Troy H, Ramirez de Molina A, Jackson LE, Madhu B, Griffiths JR, Leach MO, Workman P, Lacal JC, Judson IR, et al. (2006). Noninvasive magnetic resonance spectroscopic pharmacodynamic markers of the choline kinase inhibitor MN58b in human carcinoma models. *Cancer Res* **66,** 427–434.
[15] Meisamy S, Bolan PJ, Baker EH, Pollema MG, Le CT, Kelcz F, Lechner MC, Luikens BA, Carlson RA, Brandt KR, et al. (2005). Adding *in vivo* quantitative ^{1}H MR spectroscopy to improve diagnostic accuracy of breast MR imaging: preliminary results of observer performance study at 4.0 T. *Radiology* **236,** 465–475.
[16] Howe FA and Opstad KS (2003). ^{1}H MR spectroscopy of brain tumours and masses. *NMR Biomed* **16,** 123–131.
[17] Howe FA, Barton SJ, Cudlip SA, Stubbs M, Saunders DE, Murphy M, Wilkins P, Opstad KS, Doyle VL, McLean MA, et al. (2003). Metabolic profiles of human brain tumors using quantitative *in vivo* ^{1}H magnetic resonance spectroscopy. *Magn Reson Med* **49,** 223–232.
[18] Cheng LL, Ma MJ, Becerra L, Ptak T, Tracey I, Lackner A, and Gonzalez RG (1997). Quantitative neuropathology by high resolution magic angle spinning proton magnetic resonance spectroscopy. *Proc Natl Acad Sci USA* **94,** 6408–6413.
[19] Ratai EM, Pilkenton S, Lentz MR, Greco JB, Fuller RA, Kim JP, He J, Cheng LL, and Gonzalez RG (2005). Comparisons of brain metabolites observed by HRMAS ^{1}H NMR of intact tissue and solution ^{1}H NMR of tissue extracts in SIV-infected macaques. *NMR Biomed* **18,** 242–251.
[20] Valonen PK, Griffin JL, Lehtimaki KK, Liimatainen T, Nicholson JK, Grohn OH, and Kauppinen RA (2005). High-resolution magic-angle-spinning ^{1}H NMR spectroscopy reveals different responses in choline-containing metabolites upon gene therapy-induced programmed cell death in rat brain glioma. *NMR Biomed* **18,** 252–259.
[21] Le Belle JE, Harris NG, Williams SR, and Bhakoo KK (2002). A comparison of cell and tissue extraction techniques using high-resolution ^{1}H-NMR spectroscopy. *NMR Biomed* **15,** 37–44.
[22] Zhao M, Pipe JG, Bonnett J, and Evelhoch JL (1996). Early detection of treatment response by diffusion-weighted ^{1}H-NMR spectroscopy in a murine tumour *in vivo*. *Br J Cancer* **73,** 61–64.
[23] Chenevert TL, McKeever PE, and Ross BD (1997). Monitoring early response of experimental brain tumors to therapy using diffusion magnetic resonance imaging. *Clin Cancer Res* **3,** 1457–1466.
[24] Ross BD, Moffat BA, Lawrence TS, Mukherji SK, Gebarski SS, Quint DJ, Johnson TD, Junck L, Robertson PL, Muraszko KM, et al. (2003). Evaluation of cancer therapy using diffusion magnetic resonance imaging. *Mol Cancer Ther* **2,** 581–587.
[25] Thoeny HC, De Keyzer F, Chen F, Ni Y, Landuyt W, Verbeken EK, Bosmans H, Marchal G, and Hermans R (2005). Diffusion-weighted MR imaging in monitoring the effect of a vascular targeting agent on rhabdomyosarcoma in rats. *Radiology* **234,** 756–764.
[26] Workman P, Twentyman P, Balkwill F, Balmain A, Chaplin D, Double J, Embleton J, Newell D, Raymond R, Stable J, et al. (1998). United Kingdom Co-ordinating Committee on Cancer Research (UKCCCR) Guidelines for the Welfare of Animals in Experimental Neoplasia (Second Edition). *Br J Cancer* **77,** 1–10.
[27] Twentyman PR, Brown JM, Gray JW, Franko AJ, Scoles MA, and Kallman RF (1980). A new mouse tumor model system (RIF-1) for comparison of end-point studies. *J Natl Cancer Inst* **64,** 595–604.
[28] de Graaf RA and Rothman DL (2001). *In vivo* detection and quantification of scalar coupled ^{1}H NMR resonances. *Concepts Magn Reson* **13,** 32–76.
[29] van der Veen JW, de Beer R, Luyten PR, and van Ormondt D (1988). Accurate quantification of *in vivo* ^{31}P NMR signals using the variable projection method and prior knowledge. *Magn Reson Med* **6,** 92–98.
[30] Vanhamme L, van den Boogaart A, and Van Huffel S (1997). Improved method for accurate and efficient quantification of MRS data with use of prior knowledge. *J Magn Reson* **129,** 35–43.
[31] Klose U (1990). *In vivo* proton spectroscopy in presence of eddy currents. *Magn Reson Med* **14,** 26–30.
[32] Bennett KM, Schmainda KM, Bennett RT, Rowe DB, Lu H, and Hyde JS (2003). Characterization of continuously distributed cortical water diffusion rates with a stretched-exponential model. *Magn Reson Med* **50,** 727–734.
[33] Braunschweiger PG (1988). Effect of cyclophosphamide on the pathophysiology of RIF-1 solid tumors. *Cancer Res* **48,** 4206–4210.
[34] Morse DL and Gillies RJ (2005). Choline containing compounds as diagnostic, prognostic and therapeutic response indicators for breast cancer. In *Recent Advances in MR Imaging and Spectroscopy*. NR Jagannathan (Ed). Jaypee Brothers Medical Publishers, New Delhi, India, pp 345–397.
[35] Podo F (1999). Tumour phospholipid metabolism. *NMR Biomed* **12,** 413–439.
[36] Glunde K, Jie C, and Bhujwalla ZM (2004). Molecular causes of the aberrant choline phospholipid metabolism in breast cancer. *Cancer Res* **64,** 4270–4276.
[37] de Molina AR, Gutiérrez R, Ramos MA, Silva JM, Silva J, Bonilla F, Sánchez JJ, and Lacal JC (2002). Increased choline kinase activity in human breast carcinomas: clinical evidence for a potential antitumour strategy. *Oncogene* **21,** 4317–4322.
[38] Maxwell RJ, Nielsen FU, Breidahl T, Stødkilde-Jørgensen H, and Horsman MR (1998). Effects of combretastatin on murine tumours monitored by ^{31}P MRS, ^{1}H MRS and ^{1}H MRI. *Int J Radiat Oncol Biol Phys* **42,** 891–894.
[39] Nielsen FU (1999). Implementation and development of ^{1}H and ^{13}C nuclear magnetic resonance spectroscopy methods for studying tumour metabolism. PhD Thesis Faculty of Health Sciences, University of Aarhus, Denmark.
[40] Halestrap AP and Denton RM (1974). Specific inhibition of pyruvate transport in rat liver mitochondria and human erythrocytes by α-cyano-4-hydroxycinnamate. *Biochem J* **138,** 313–316.
[41] Schuller-Levis GB and Park E (2003). Taurine: new implications for an old amino acid. *FEMS Microbiol Lett* **226,** 195–202.
[42] Sliarenko JV, Lunt SJ, Gordon ML, Vitkin A, Milosevic M, and Hill RP

(2006). Effects of the vascular disrupting agent ZD6126 on interstitial fluid pressure and cell survival in tumors. *Cancer Res* **66,** 2074–2080.

[43] Robinson SP, Kalber TL, Howe FA, McIntyre DJ, Griffiths JR, Blakey DC, Whittaker L, Ryan AJ, and Waterton JC (2005). Acute tumor response to ZD6126 assessed by intrinsic susceptibility magnetic resonance imaging. *Neoplasia* **7,** 466–474.

[44] Vogel-Claussen J, Gimi B, and Bhujwalla ZM (2005). Diffusion-weighted MRI detects early treatment response after antivascular therapy of prostate tumours. In *Proceedings of the 13th Annual Meeting of the International Society for Magnetic Resonance in Medicine,* Miami Beach, USA, p 2127.

[45] Leach MO, Brindle KM, Evelhoch JL, Griffiths JR, Horsman MR, Jackson A, Jayson G, Judson IR, Knopp MV, Maxwell RJ, et al. (2005). The assessment of antiangiogenic and antivascular therapies in early-stage clinical trials using magnetic resonance imaging: issues and recommendations. *Br J Cancer* **92,** 1599–1610.

[46] Beauregard DA, Pedley RB, Hill SA, and Brindle KM (2002). Differential sensitivity of two adenocarcinoma xenografts to the anti-vascular drugs combretastatin A4 phosphate and 5,6-dimethylxanthenone-4-acetic acid, assessed using MRI and MRS. *NMR Biomed* **15,** 99–105.

[47] Briedahl T, Nielsen FU, Stødkilde-Jørgensen H, Maxwell RJ, and Horsman MR (2006). The effects of the vascular disrupting agents combretastatin A-4 disodium phosphate, 5,6-dimethylxanthenone-4-acetic acid and ZD6126 in a murine tumour: a comparative assessment using MRI and MRS. *Acta Oncol* **45,** 306–316.

[48] Jordan BF, Black K, Robey IF, Runquist M, Powis G, and Gillies RJ (2005). Metabolite changes in HT-29 xenograft tumors following HIF-1α inhibition with PX-478 as studied by MR spectroscopy *in vivo* and *ex vivo*. *NMR Biomed* **18,** 430–439.

[49] Chung YL, Troy H, Banerji U, Jackson LE, Walton MI, Stubbs M, Griffiths JR, Judson IR, Leach MO, Workman P, and Ronen SM (2003). Magnetic resonance spectroscopic pharmacodynamic markers of the heat shock protein 90 inhibitor 17-allylamino,17-demethoxygeldanamycin (17AAG) in human colon cancer models. *J Natl Cancer Inst* **95,** 1624–1633.